Published OnlineFirst January 10, 2011; DOI:10.1158/1078-0432.CCR-10-2132

suggests that this miRNA primarily achieves its antiproliferative effect through downregulation of proliferation-related genes, including *ERBB2*, a member of the EGF receptor family of receptor tyrosine kinases, which regulate a key initiator of phosphoinositide-3 kinase (PI3K)-AKT and RAS/RAF/mitogen-activated protein kinase signaling (28). *miR-125a-5p* is shown to be a superior biomarker to previously reported gastric cancer biomarkers such as *DACH1* and *PDCD6* (ref. 22; Supplementary Table S1). However, because of the differences in patient backgrounds such as clinical stage and the presence or absence of chemotherapy, further investigation is required for adequate use of these biomarkers.

We confirmed *miR-125a–ERBB2* interaction in the human gastric cancer cell line NUGC4. *MiR-125a-5p* significantly repressed ERBB2 expression and the phosphorylation of its downstream molecule, AKT (Fig. 3B). In addition, *ERBB2* expression was shown to be inversely correlated with expression of *miR-125a-5p* both *in vitro* and in clinical samples. Overexpression of *Pre-miR-125a* also led to the inhibition of previously reported *miR-125a-5p* targets, such as apoptosis-related gene *BAK1* (26) and tumor suppressor gene *p53* (ref. 27; Supplementary Fig. S3). However, the inhibition of these tumor suppressor genes was modest compared with that of ERBB2, suggesting ERBB2 is a crucial target of *miR-125a-5p*, at least in the gastric cancer cell line NUGC4.

It is noteworthy that the growth inhibitory effect of *miR-125a-5p* was enhanced when combined with trastuzumab (Fig. 4A and B). This could be partly due to the fact that *miR-125a-5p* and trastuzumab share the same target, *ERBB2*. *miR-125a-5p* and trastuzumab silence the *ERBB2* pathway through 2 different mechanisms. *miR-125a-5p* suppresses the molecule at the posttranscriptional level before protein synthesis, whereas trastuzumab is a monoclonal antibody targeted against completed ERBB2 protein. In other words, *miR-125a-5p* blocks the synthesis of the oncoprotein at an earlier phase than does trastuzumab. These considerations suggest that *miR-125a-5p* mimic and trastuzumab have the potential to be highly effective against ERBB2 when used together.

ERBB2-positive gastric cancer patients constitute about 19.0% (8.2%–53.4%) of all gastric cancer patients (19, 29, 30). A recent phase III study (the ToGA trial) combining treatment of trastuzumab and conventional chemotherapy against ERBB2-positive gastric cancer showed a statistically significant advantage in overall survival for patients who received combined therapy compared with chemotherapy alone. These reliable large-scale clinical data indicate that ERBB2 is a crucial therapeutic target in gastric cancer (31).

In conclusion, our data suggest that *miR-125a-5p* functions as a powerful tumor suppressor and could be a bona fide prognostic marker for gastric cancer patients. Furthermore, *miR-125a-5p* mimic alone or in combination with trastuzumab could be a novel therapeutic approach against gastric cancer.

Disclosure of Potential Conflicts of Interest

No potential conflicts of interest were disclosed.

Acknowledgments

We thank T. Shimooka, K. Ogata, M. Kasagi, and T. Kawano for their excellent technical assistance.

Grant Support

This work was supported in part by the following grants and foundations: CREST, Japan Science and Technology Agency (JST); Japan Society for the Promotion of Science (JSPS) Grant-in-Aid for Scientific Research: 21679006, 20390360, 20590313, 20591547, 21591644, 21592014, 20790960, 21791297, 21229015, 20659209, and 20012039; NEDO (New Energy and Industrial Technology Development Organization) Technological Development for Chromosome Analysis; The Ministry of Education, Culture, Sports, Science and Technology of Japan for Scientific Research on Priority Areas, Cancer Translational Research Project, Japan.

The costs of publication of this article were defrayed in part by the payment of page charges. This article must therefore be hereby marked *advertisement* in accordance with 18 U.S.C. Section 1734 solely to indicate this fact.

Received August 7, 2010; revised December 6, 2010; accepted December 18, 2010; published online May 2, 2011.

References

1. Bartel DP. MicroRNAs: target recognition and regulatory functions. Cell 2009;136:215–33.
2. Nicoloso MS, Spizzo R, Shimizu M, Rossi S, Calin GA. MicroRNAs—the micro steering wheel of tumour metastases. Nat Rev Cancer 2009;9:293–302.
3. Spizzo R, Nicoloso MS, Croce CM, Calin GA. SnapShot: microRNAs in cancer. Cell 2009;137:586–e1.
4. Guo X, Wu Y, Hartley RS. MicroRNA-125a represses cell growth by targeting HuR in breast cancer. RNA Biol 2009;6:575–83.
5. Li W, Duan R, Kooy F, Sherman SL, Zhou W, Jin P. Germline mutation of microRNA-125a is associated with breast cancer. J Med Genet 2009;46:358–60.
6. O'Day E, Lal A. MicroRNAs and their target gene networks in breast cancer. Breast Cancer Res 2010;12:201.
7. Nam EJ, Yoon H, Kim SW, Kim H, Kim YT, Kim JH, et al. MicroRNA expression profiles in serous ovarian carcinoma. Clin Cancer Res 2008;14:2690–5.
8. Wang G, Mao W, Zheng S, Ye J. Epidermal growth factor receptor-regulated miR-125a-5p—a metastatic inhibitor of lung cancer. FEBS J 2009;276:5571–8.
9. Ferretti E, De Smaele E, Po A, Di Marcotullio L, Tosi E, Espinola MS, et al. MicroRNA profiling in human medulloblastoma. Int J Cancer 2009;124:568–77.
10. Cowden Dahl KD, Dahl R, Kruichak JN, Hudson LG. The epidermal growth factor receptor responsive miR-125a represses mesenchymal morphology in ovarian cancer cells. Neoplasia 2009;11:1208–15.
11. Park NJ, Zhou H, Elashoff D, Henson BS, Kastratovic DA, Abemayor E, et al. Salivary microRNA: discovery, characterization, and clinical utility for oral cancer detection. Clin Cancer Res 2009;15:5473–7.
12. Scott GK, Goga A, Bhaumik D, Berger CE, Sullivan CS, Benz CC. Coordinate suppression of ERBB2 and ERBB3 by enforced expression of micro-RNA miR-125a or miR-125b. J Biol Chem 2007;282:1479–86.
13. Gravalos C, Jimeno A. HER2 in gastric cancer: a new prognostic factor and a novel therapeutic target. Ann Oncol 2008;19:1523–9.

Published OnlineFirst January 10, 2011; DOI:10.1158/1078-0432.CCR-10-2132

14. Marx AH, Tharun L, Muth J, Dancau AM, Simon R, Yekebas E, et al. HER-2 amplification is highly homogenous in gastric cancer. Hum Pathol 2009;40:769–77.
15. Kim SY, Kim HP, Kim YJ, Oh do Y, Im SA, Lee D, et al. Trastuzumab inhibits the growth of human gastric cancer cell lines with HER2 amplification synergistically with cisplatin. Int J Oncol 2008;32:89–95.
16. Matsui Y, Inomata M, Tojigamori M, Sonoda K, Shiraishi N, Kitano S. Suppression of tumor growth in human gastric cancer with HER2 overexpression by an anti-HER2 antibody in a murine model. Int J Oncol 2005;27:681–5.
17. Japanese Gastric Cancer Association. Japanese Classification of Gastric Carcinoma—2nd English edition. Gastric Cancer 1998;1:10–24.
18. Aihara H, Kawamura YJ, Toyama N, Mori Y, Konishi F, Yamada S, et al. Analysis of the gene-expression profile regarding the progression of human gastric carcinoma. Surgery 2002;131:S39–47.
19. Hofmann M, Stoss O, Shi D, Büttner R, van de Vijver M, Kim W, et al. Assessment of a HER2 scoring system for gastric cancer: results from a validation study. Histopathology 2008;52:797–805.
20. Rüschoff J, Dietel M, Baretton G, Arbogast S, Walch A, Monges G, et al. HER2 diagnostics in gastric cancer—guideline validation and development of standardized immunohistochemical testing. Virchows Arch 2010;457:299–307.
21. Blower PE, Verducci JS, Lin S, Zhou J, Chung JH, Dai Z, et al. MicroRNA expression profiles for the NCI-60 cancer cell panel. Mol Cancer Ther 2007;6:1483–91.
22. Yamada Y, Arao T, Gotoda T, Taniguchi H, Oda I, Shirao K, et al. Identification of prognostic biomarkers in gastric cancer using endoscopic biopsy samples. Cancer Sci 2008;99:2193–9.
23. Betel D, Wilson M, Gabow A, Marks DS, Sander C. The microRNA.org resource: targets and expression. Nucleic Acids Res 2008;36:D149–53.
24. Krek A, Grün D, Poy MN, Wolf R, Rosenberg L, Epstein EJ, et al. Combinatorial microRNA target predictions. Nat Genet 2005;37:495–500.
25. Lewis BP, Burge CB, Bartel DP. Conserved seed pairing, often flanked by adenosines, indicates that thousands of human genes are microRNA targets. Cell 2005;120:15–20.
26. Guo S, Lu J, Schlanger R, Zhang H, Wang JY, Fox MC, et al. MicroRNA miR-125a controls hematopoietic stem cell number. Proc Natl Acad Sci U S A 2010;107:14229–34.
27. Zhang Y, Gao JS, Tang X, Tucker LD, Quesenberry P, Rigoutsos I, et al. MicroRNA 125a and its regulation of the p53 tumor suppressor gene. FEBS Lett 2009;583:3725–30.
28. Hsieh AC, Moasser MM. Targeting HER proteins in cancer therapy and the role of the non-target HER3. Br J Cancer 2007;97:453–7.
29. Allgayer H, Babic R, Gruetzner KU, Tarabichi A, Schildberg FW, Heiss MM. c-erbB-2 is of independent prognostic relevance in gastric cancer and is associated with the expression of tumor-associated protease systems. J Clin Oncol 2000;18:2201–9.
30. Jorgensen JT. Targeted HER2 treatment in advanced gastric cancer. Oncology 2010;78:26–33.
31. Bang YJ, Van Cutsem E, Feyereislova A, Chung HC, Shen L, Sawaki A, et al. Trastuzumab in combination with chemotherapy versus chemotherapy alone for treatment of HER2-positive advanced gastric or gastro-oesophageal junction cancer (ToGA): a phase 3, open-label, randomised controlled trial. Lancet 2010;376:687–97.

Ann Surg Oncol (2011) 18:261–272
DOI 10.1245/s10434-010-1271-1

Annals of
SURGICAL ONCOLOGY
OFFICIAL JOURNAL OF THE SOCIETY OF SURGICAL ONCOLOGY

ORIGINAL ARTICLE – TRANSLATIONAL RESEARCH AND BIOMARKERS

STC2: A Predictive Marker for Lymph Node Metastasis in Esophageal Squamous-Cell Carcinoma

Yoshiaki Kita, MD, PhD[1,2], Koshi Mimori, MD, PhD[1], Masaaki Iwatsuki, MD, PhD[1], Takehiko Yokobori, MD, PhD[1], Keisuke Ieta, MD, PhD[1], Fumiaki Tanaka, MD, PhD[1], Hideshi Ishii, MD, PhD[1], Hiroshi Okumura, MD, PhD[2], Shoji Natsugoe, MD, PhD[2], and Masaki Mori, MD, PhD, FACS[3]

[1]Department of Surgery, Medical Institute of Bioregulation, Kyushu University, Beppu, Japan; [2]Department of Surgical Oncology and Digestive Surgery, Field of Oncology, Course of Advanced Therapeutics, Kagoshima University Graduate School of Medical and Dental Science, Kagoshima, Japan; [3]Department of Gastroenterological Surgery, Graduate School of Medicine, Osaka University, Suita, Japan

ABSTRACT

Background. We sought to identify genes associated with the progression and metastasis of esophageal squamous-cell cancer by comparing the expression profiles of normal, primary cancer, and metastatic cancer cells isolated with laser microdissection.

Methods. Oligo microarray analysis identified several lymph node-specific, metastasis-related genes. *STC2* (stanniocalcin 2), which was overexpressed in esophageal cancer cases, was chosen for further characterization. Quantitative reverse transcriptase-polymerase chain reaction and immunohistochemistry were used to explore the clinicopathologic significance of *STC2* expression status in 70 cases. Additionally, the functional role of *STC2* in esophageal cancer was studied by the attenuation of *STC2* in an esophageal cancer cell line.

Results. Laser microdissection and oligo microarray analysis identified 63 candidate genes. Among them, *STC2* showed higher expression in cancer tissue than in corresponding normal tissue ($P < 0.001$). *STC2* expression was significantly correlated with lymph node metastasis, lymphatic invasion, and distant metastasis ($P = 0.005$, 0.007, and 0.038, respectively). Patients whose tumors had high *STC2* expression had a worse 5-year survival rate than patients whose tumors had a low *STC2* expression level ($P = 0.016$). *STC2* transfected cells had a significantly higher proliferation rate than control cells ($P < 0.001$). Additionally, *STC2* transfected cells were more invasive in vitro ($P < 0.001$) than control cells. These findings were validated by means of RNA interference assays.

Conclusions. We identified lymph node-specific, metastasis-related genes in esophageal cancer cells. One of these, *STC2*, may be associated with lymph node metastasis, making it a potential prognostic marker for esophageal cancer patients.

First Received: 24 January 2010;
Published Online: 24 August 2010

M. Mori, MD, PhD, FACS
e-mail: kmimori@beppu.kyushu-u.ac.jp

Esophageal squamous-cell cancer (ESC) is one of the most intractable gastrointestinal tract cancers.[1,2] Finding a cure for this malignancy rests on the identification of genetic and molecular markers of malignancy potential, which could serve as specific treatment targets. However, the regulation of complex processes over multiple events precludes the identification of practical markers for carcinogenesis, tumor progression, and metastasis.

Numerous genes modulate the signaling cascades that accelerate these processes. Tumor behavior is also affected by the multiple cell types in primary tumors that consist of interstitial tissues, macrophages, and lymphocytes in addition to cancer cells. Therefore, the goal of this study was to use laser micro-dissection (LMD) to focus on gene expression profiles of cancer cells. Use of this technological innovation has revealed the activity of genes with previously unknown functions in gastric,[3,4] colon[5] and breast cancers.[6]

In this study, in microarray gene expression profiles of cancer-specific genes involved in cancer progression, stanniocalcin 2 (*STC2*), a homologue of a glycoprotein hormone originally found to regulate calcium/phosphate homeostasis in bony fish, was abundantly expressed in esophageal cancers with lymph nodes metastasis.[7] *STC2* was subsequently classified as a possible prognostic

marker, and its effects on cell proliferation and invasiveness were validated in vitro via transfection of *STC* into an esophageal cancer cell line.

A precise predictive marker for lymph node metastasis would allow small pieces of primary tumors to be used in determining the necessity of radical lymph node dissection through the thoracotomy. *STC2* was reported to be associated with breast cancer, ovarian cancer, renal-cell carcinoma, prostate cancer, and neuroblastoma.[8–14] However, the expression of *STC2* and biological behavior in ESC has not been evaluated. This study unveiled an intriguing role for *STC2* in the progression and malignancy of esophageal cancer.

MATERIALS AND METHODS

Tissue Sampling

All clinical samples obtained in Kagoshima University Hospital were sent to our institute. Microarray samples of tumor and noncancerous adjacent tissues were collected from five male patients with esophageal cancer who underwent esophagectomy with lymph node dissection at Kagoshima University Hospital, Japan. Average age was 64.6 (range 49–76) years. There were two cases of well-differentiated ESC, two moderately differentiated ESC, and one poorly differentiated ESC. All cases were positive for lymph node metastases; no distant metastasis was present. All patients provided informed consent in accordance with the institutional guidelines of the hospitals at Kyushu University and Kagoshima University. We used the tumor, node, metastasis system classification developed by the International Union Against Cancer.[15]

Collection of Target Cells by LMD from Frozen Sections

Frozen section slides were fixed in 70% ethanol for 30 seconds and stained with hematoxylin and eosin before dehydration (5 seconds each in 70%, 95%, and 100% ethanol). After air drying, the sections were laser microdissected with a LMD system (Leica Microsystems, Wezlar, Germany) (Fig. 1a). Target cells were excised, at least 100 cells per section, and bound to the transfer film. Fifteen sections were collected from every sample; thus, approximately 10,000 to 15,000 cells were collected from each sample for total RNA extraction.

RNA Extraction and Oligonucleotide Microarray Analysis

RNA extraction was performed as described previously.[16,17] The commercially available Human Whole Genome Oligo Microarray Kit (Agilent Technologies, Palo Alto, CA), which contains more than 41,000 features, including 36,866 characterized human genes, was used for microarray analysis (http://www.chem.agilent.com/scripts/generic.asp?lpage=5175&indcol=Y&prodcol=Y). The microarray study followed the MIAME guidelines issued by the Microarray Gene Expression Data group.[18] Differences in the expression profiles between the primary esophageal cancer cells (T) and the normal squamous cells (N), and between the primary esophageal cancer cells (T) and metastatic cancer cells from lymph nodes (M) were evaluated by comparing the average intensities. To reduce the false discovery rate, the Benjamini and Hochberg adjustment for multiple hypothesis comparisons was used.[19]

Esophageal Cancer Cell Lines

The human esophageal cancer cell lines KYSE70 and TE13 were obtained from the Cell Resource Center for Biomedical Research Institute of Development, Aging and Cancer (Tohoku University, Sendai, Japan). They were maintained in RPMI 1640 medium containing 10% fetal bovine serum and antibiotics at 37°C in a 5% humidified CO_2 atmosphere.

Real-Time Quantitative Reverse Transcription-Polymerase Chain Reaction

Real-time quantitative reverse transcriptase-polymerase chain reaction (RT-PCR) was performed on an additional 70 surgical esophageal cancer specimens with paired normal samples that were not used in the microarray analysis. Total RNA was extracted from each bulk sample, and cDNA was synthesized from total RNA as described previously.[20] The following primers were used to amplify the *STC2* gene: sense primer, 5′-TCAAAGACGCCTTGAAA TGTAA-3′; antisense primer, 5′-CAGTTCTGCTCACAC TGAACCT-3′. The glyceraldehyde-3-phosphate dehydrogenase (*GAPDH:* sense primer, 5′-TTGGTATCGTGGA AGGACTCA-3′; antisense primer, 5′-TGTCATCATATT TGGCAGGTT-3′) gene was used as an internal control. Real-time monitoring of PCR reactions was performed with the Light-Cycler System (Roche Applied Science, Indianapolis, IN) and SYBR green I dye (Roche). Details for each reaction are described elsewhere.[21] Each assay was performed in triplicate.

Immunohistochemistry

STC2 expression was localized on formalin-fixed, paraffin-embedded surgical specimens from esophageal cancer patients by the avidin–biotin–peroxidase method (LSAB2 Kit; Dako, Kyoto, Japan).[5] All sections were counterstained

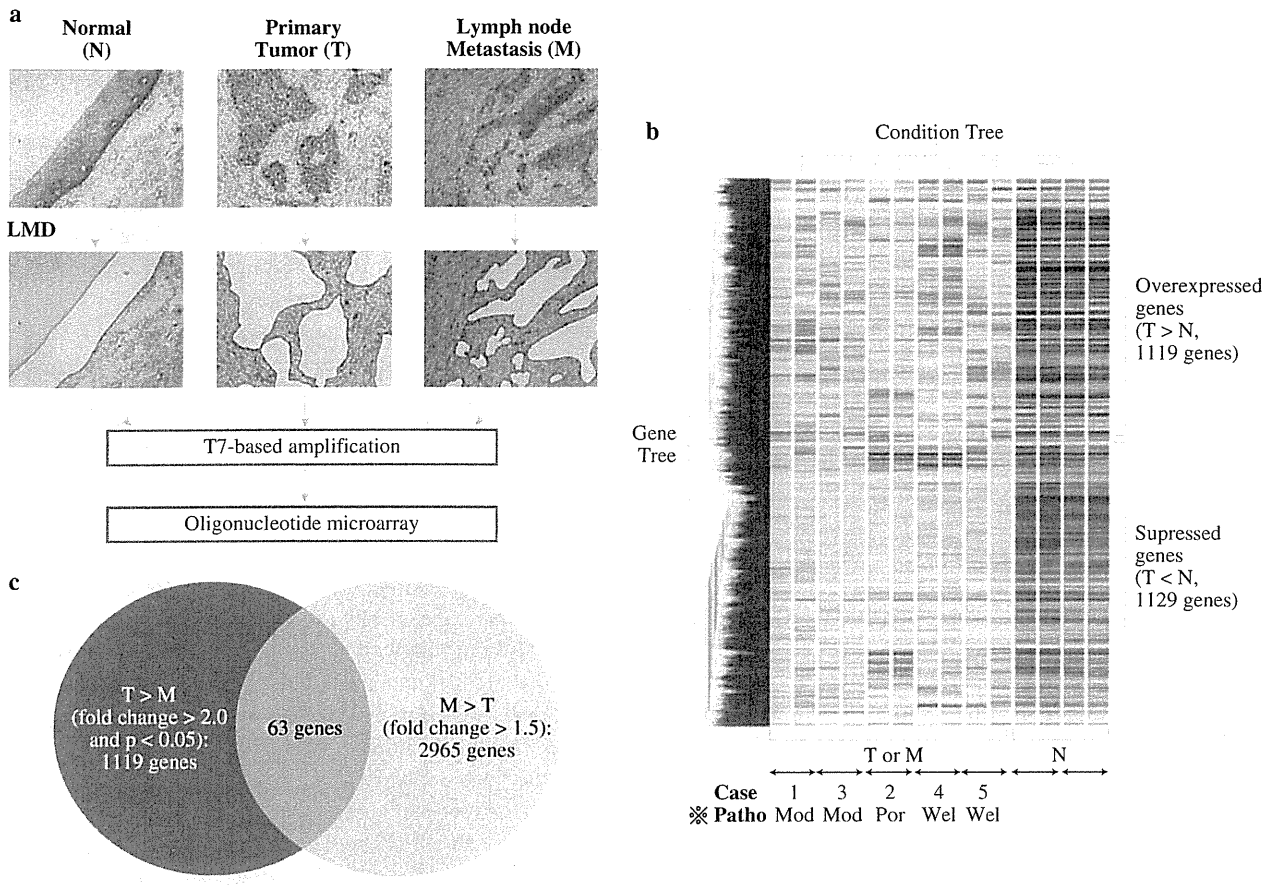

FIG. 1 **a** A schema of the laser microdissection (LMD), T7 linear amplification, and oligonucleotide microarray. Primary esophageal squamous-cell cancer (ESC) cells, metastatic cancer cells, and normal squamous cells were obtained by LMD. After the extraction of total RNA, T7-based amplification was performed, followed by oligonucleotide microarray analysis. **b** Hierarchical clustering analysis using 2248 differentially expressed genes between primary ESC cells (T) and normal squamous cells (N) ($P < 0.05$). The cancer cells (T and M) and normal squamous cells were classifiable, whereas the expression patterns of T and M were indistinguishable. **c** Sixty-three genes extracted from the 1119 genes were upregulated by primary ESC cells (T) compared with normal squamous cells (N), and 2965 genes were upregulated by metastatic cancer cells from lymph nodes (M) compared with primary ESC cells (T)

with hematoxylin. A primary mouse monoclonal antibody against *STC2* (STC2; Abnova, Taiwan) was used at a dilution of 1:500.

Stable Transfection of STC2 Into Esophageal Cancer Cell Line

Human *STC2* cDNA was generated by RT-PCR and subcloned into the pcDNA3.1/Hygro expression vector (Invitrogen, Carlsbad, CA) according to the manufacturer's protocol. Sequencing confirmed accurate reading frame insertion. Transfection into an esophageal cancer cell line (KYSE70) lacking expression of the STC2 protein was performed with Lipofectamine2000 (Invitrogen), as described previously.[22] Stable transfectants expressing abundant STC2 protein were selected by G418 (Invitrogen) treatment and used for subsequent experiments. A mock-transfected clone was used as the control.

STC2 RNA Interference

STC2-specific siRNA (Stealth siRNA duplex oligoribonucleotides) and negative control RNAi (Stealth Negative Control siRNA duplex oligoribonucleotides) were purchased from Invitrogen. Logarithmically growing cells (TE13) were seeded at either 1.0×10^5 or 2.0×10^3 cells per well in a final volume of 2 mL or 100 μL in 6- or 96-well flat-bottom microplates, respectively. The cells were cultured overnight for adherence. RNAi Oligomer was diluted with Opti-MEN I Reduced Serum Medium (Invitrogen) and incubated for 5 minutes at room temperature. The diluted RNAi oligomer was mixed with diluted

Lipofectamine RNAi MAX (Invitrogen). The RNAi–Lipofectamine RNAi MAX complexes were added to each well at a final concentration of 30 pmol/mL. The cells were incubated for 5 hours, followed by replacement of the media. The assays were performed after a 48-hour incubation.

Western Blot Analysis

Western blot analysis was used to confirm the expression of *STC2* in KYSE70 cells transfected with *STC2* or the mock vector, and TE13 cells transfected with either *STC2*-specific RNAi or negative control RNAi. Total protein was extracted from samples with Pro-Prep protein extraction solution (iNtRON Biotechnology, Korea).

In Vitro Proliferation Assays

Proliferation was determined with a MTT (3-(4,5-dimethylthiazol-2-yl)-2,5-diphenyltetrazolium bromide) assay (Roche). Logarithmically growing cells were seeded at 5.0×10^3 cells/well in flat-bottomed 96-well microtiter plate in a final volume of 100 μL culture medium per well and incubated in a humidified atmosphere (37°C and 5% CO_2). MTT labeling reagent (10 μL at a final concentration of 0.5 mg/mL) was then added to each well. The microtiter plate was incubated for 4 hours in a humidified atmosphere, after which solubilization solution (100 μL) was added to each well. The plate was then incubated overnight in a humidified atmosphere. Once complete solubilization of the purple formazan crystals was confirmed, the absorbance of the samples was measured with a microplate reader (model 550; Bio-Rad Laboratories, Hercules, CA) at a wavelength of 570 nm corrected to 655 nm. Each independent experiment was performed in triplicate.

In Vitro Invasion Assay

In vitro invasion assays were performed with the BD Biocort Tumor Invasion System (Becton Dickinson, San Jose, CA). Cells (5.0×10^4 cells/well) were placed in the upper chamber, and the lower chamber was filled with 750 μL of RPMI 1640 with 10% fetal bovine serum as a chemoattractant. After 72 hours of incubation at 37°C, the membranes were labeled with Calcein AM solution. The invasive cells that had migrated through the membrane to the lower surface were read in a fluorescence plate reader at excitation/emission wavelengths of 485/530 nm with a multilabel plate counter (Victor3; PerkinElmer, Waltham, MA).

Statistical Analysis

The statistical analysis of group differences was performed by the χ^2 test, the Student's *t*-test, and the repeated ANOVA test. Overall survival curves were plotted according to the Kaplan-Meier method, with the Wilcoxon test applied for comparisons. $P < 0.05$ was considered statistically significant. Variables with a value of $P < 0.05$ by univariate analysis were used in subsequent multivariate analyses based on Cox's proportional hazard model. All statistical analyses were performed by JMP for Windows, version 5.0.1 (SAS Institute, Cary, NC).

RESULTS

Comparison of Expression Profiles Between Primary ESC Cells and Normal Squamous Cells

A two-dimensional hierarchical clustering analysis showed that cancer cells (T and M) and normal squamous cells (N) could be well classified were highly distinguishable, whereas the expression patterns between primary ESC cells (T) and metastatic cancer cells in the lymph nodes (M) were indistinguishable. Interestingly, for each case the gene expression pattern of the primary ESC cells (T) and the metastatic cancer cells from the lymph nodes of the same patient (M) was distinguishable from that of normal squamous cells (N) (Fig. 1b). Four of the five samples from the microdissected normal sections and all five samples from the microdissected primary and metastatic cancers were determined to be of sufficient quality to proceed with analysis.

Once background correction and normalization were complete, unwanted genes were filtered out. Genes with intensities near the level of background noise (10,825 of 41,134) were removed first (as described in "Materials and Methods"). Second, the 28,061 genes with fold changes between 0.5 and 2.0, and those determined not significant by the ANOVA test with the Benjamini and Hochberg adjustment for individual comparison were removed. Of the remaining 2248 genes, 1119 were upregulated and 1129 were downregulated in primary esophageal cancer cells compared with normal squamous cells (Fig. 1c).

Comparison of Expression Profiles Between Primary Cancer Cells and Metastatic Cancer Cells from Lymph Nodes (M)

The gene expression profiles of primary ESC cells and metastatic cancer cells in the lymph nodes (M) were so similar that statistically significant genes could not be identified. Therefore, only the fold change method was used; 25,209 genes with fold changes between 0.77 and 1.5

TABLE 1 Overexpressed genes correlated with lymph node metastasis

Gene symbol	GenBank accession no.	Description
Cell adhesion		
SPP1	NM_000582	Secreted phosphoprotein 1 (osteopontin)
TACSTD1	NM_002354	Tumor-associated calcium signal transducer 1
CDHB11	NM_018931	Protocadherin beta 11
PKD2	NM_000297	Polycystic kidney disease 2 (autosomal dominant)
BHLHB2	NM_030762	Basic helix-loop-helix domain containing, class B,3
ICAM1	NM_000201	Intercellular adhesion molecule 1 (CD54), human rhinovirus receptor
Cell cycle		
KNTC1	NM_014708	Kinetochore-associated 1
INHBA	NM_002192	Inhibin, beta A (activin A, activin AB alpha polypeptide)
RBM22	NM_018047	RNA binding motif protein 22
TERF1	NM_017489	Telomeric repeat binding factor (NIMA interacting) 1
KIF11	NM_004523	Kinesin family member 11
KNTC2	NM_006101	Kinetochore associated 2
Cell differntination		
CDK5RAP2	NM_018249	CDK5 regulatory subunit associated protein 2
Cell division		
SMC2	NM_006444	SMC2 structural maintenance of chromosomes 2-like 1 (yeast)
Cell growth/proliferation		
PTPRJ	BC019824	Protein tyrosine phosphatase, receptor type, J
PMP22	NM_000304	Peripheral myelin protein 22
PRAME	NM_206956	Preferentially expressed antigen in melanoma
Cell–cell signaling		
STC2	NM_003714	Stanniocalcin 2
MDK	NM_001012334	Midkine (neurite growth-promoting factor 2)
Inflammatory		
PLA2G7	NM_005084	Phospholipase A2, group VII (platelet-activating factor acetylhydrolase)
Metabolism		
SDF4	NM_016176	Stromal cell derived factor 4
BCAT1	NM_005504	Branched chain aminotransferase 1
APOC1	NM_001645	Apolipoprotein C-I
APOE	NM_000041	Apolipoprotein E
MTHFD2	NM_006636	Methylenetetrahydrofolate dehydrogenase (NADP+ dependent) 2
SULF1	NM_015170	Sulfatase 1
DHRS8	NM_016245	Dehydrogenase/reductase (SDR family) member 8
SMYD3	NM_022743	SET and MYND domain containing 3
Modification		
SMYD3	NM_022743	SET and MYND domain containing 3
Nerve development		
PPT1	NM_000310	Palmitoyl-protein thioesterase 1 (ceroid-lipofuscinosis, neuronal 1, infantile)
LUM	NM_002345	Lumican
Protein folding		
PDIA5	NM_006810	Protein disulfide isomerase family A, member 5
HSP90AA1	NM_005348	Heat-shock 90-kDa protein 1, alpha
Proteolysis		
FAP	NM_004460	Fibroblast activation protein, alpha
MMP12	CR603756	Matrix metallopeptidase 12 (macrophage elastase)
CTSL	NM_001912	Cathepsin L
RNA processing		
SR140	BC006474	U2-associated SR140 protein

TABLE 1 continued

Gene symbol	GenBank accession no.	Description
Signal transduction		
CXCR1	NM_020311	Chemokine orphan receptor 1
GPR161	NM_153832	G protein-coupled receptor 161
TPM1	NM_000366	Tropomyosin 1 (alpha)
MS4A4A	NM_024021	Membrane-spanning 4-domains, subfamily A, member 4
LILRB3	NM_006864	Leukocyte immunoglobulin-like receptor, subfamily B (with TM and ITIM domains), member 3
LSG1	NM_018385	Large subunit GTPase 1 homolog (*S. cerevisiae*)
Transcription		
OSR2	NM_053001	Odd-skipped related 2 (*Drosophila*)
PSIP1	NM_033222	PC4 and SFRS1 interacting protein 1
TBX3	NM_016569	T-box 3 (ulnar mammary syndrome)
NFE2L1	AL833530	Nuclear factor (erythroid-derived 2)-like 1
ZBTB26	AB046792	Zinc finger and BTB domain containing 26
SOX4	AW946823	SRY (sex determining region Y)-box 4
SMAD1	NM_005900	SMAD, mothers against DPP homolog 1 (*Drosophila*)
HEY1	NM_012258	Telomeric repeat binding factor (NIMA-interacting) 1
RELB	NM_006509	V-rel reticuloendotheliosis viral oncogene homolog B
Transport		
VIM	NM_003380	Vimentin
CEP290	NM_025114	Centrosome protein cep290
MAPK8IP3	NM_033392	Mitogen-activated protein kinase 8 interacting protein 3
Tumor supressor		
BCL7A	NM_020993	B-cell CLL/lymphoma 7A
Unknown		
TMEM39A	NM_018266	Transmembrane protein 39A
VPS13C	NM_017684	Vacuolar protein sorting 13C (yeast)
FAM111A	NM_022074	FLJ22794 protein
	BE537483	Full-length insert cDNA YH99G08, CDNA clone IMAGE:5276760
SCCPDH	NM_016002	Saccharopine dehydrogenase (putative)
PTDSS1	NM_014754	Phosphatidylserine synthase 1
IGF2BP2	NM_006548	IGF-II mRNA-binding protein 2
HSPBAP1	NM_024610	HSPB (heat-shock 27-kDa) associated protein 1
WDR66	NM 144668WD	Repeat domain 66

were excluded. Of the remaining 5100 genes, 2965 were upregulated and 2135 genes were downregulated in metastatic cancer cells from the lymph nodes (M) compared with primary ESC cells (Fig. 1c).

Candidate Lymph Node-Specific, Metastasis-Related Genes

We extracted 63 genes that overlapped the 1119 genes that were upregulated in primary ESC cells (T) and the 2965 genes upregulated by metastatic cancer cells in the lymph nodes (Fig. 1c; Table 1). Moreover, we selected and analyzed one of the 63 genes, *STC2,* as it was correlated with clinicopathological variables in ESC.

Identification of STC2-Associated Genes that Influence the Progression of Esophageal Cancer

To comprehend the definitive function of *STC2* in the progression of esophageal cancer, we performed oligo microarray analysis to find genes with a significant association with *STC2* expression (Table 2). Two probes were located in the coding region of *STC2* (A_23_P110686 and A_23_P416395; Affimetrix, Tokyo, Japan). Among 11 upregulated genes commonly correlated with two independent probes in *STC2,* six probes in the solute carrier family 7 (cationic amino acid transporter, y+ system) member 11 (*SLC7A11*) were significantly associated with two different probes. Notch 3 exhibited the highest *P* value

TABLE 2 Correlated gene probes associated with two independent coding regions in stanniocalcin 2 by oligo microarray analysis

Probes no.	Symbol	Description	GenBank accession no.	Cytoband	UniGene	Correlation coefficient	*P*
2	*NOTCH3*	Notch homolog 3 (*Drosophila*)	AW138903	19p13.2–p13.1	Hs.8546	0.57218	3.44E−07*
6	*SLC7A11*	Solute carrier family 7, (cationic amino acid transporter, y+ system) member 11	NM_014331	4q28–q32	Hs.390594	0.556619	8.27E−07*
2	*MAFG*	V-maf musculoaponeurotic fibrosarcoma oncogene homolog G	NM_002359	17q25.3	Hs.252229	0.555186	8.94E−07*
2	*G6PD*	Glucose-6-phosphate dehydrogenase	NM_000402	Xq28	Hs.461047	0.552849	1.02E−06*
2	*TUFT1*	Tuftelin 1	AF086205	1q21	Hs.489922	0.552382	1.04E−06*
3	*PHLDB2*	Pleckstrin homology-like domain, family B, member 2	NM_145753	3q13.2	Hs.477114	0.548711	1.27E−06*
2	*RIT1*	Ras-like without CAAX 1	NM_006912	1q22	Hs.491234	0.535188	2.58E−06*
4	*NAV1*	Neuron navigator 1	NM_020443	1q32.3	Hs.585374	0.527096	3.88E−06*
2	*SLC7A5*	Solute carrier family 7 (cationic amino acid transporter, y+ system), member 5	NM_003486	16q24.3	Hs.513797	0.513554	7.51E−06*
2	*LASS4*	LAG1 homolog, ceramide synthase 4	NM_024552	19p13.2	Hs.515111	0.51289	7.75E−06*
2	*OLFM1*	Olfactomedin 1	NM_014279	9q34.3	Hs.522484	0.511413	8.32E−06*
2	*WDR78*	WD repeat domain 78	NM_024763	1p31.3	Hs.49421	−0.578575	2.37E−07*
2	*ACSM3*	Acyl-CoA synthetase medium-chain family member 3	NM_202000	16p13.11	Hs.706754	−0.53411	2.72E−06*
2	*LZTFL1*	Leucine zipper transcription factor-like 1	NM_020347	3p21.3	Hs.30824	−0.518329	5.97E−06*
2	*TBC1D1*	TBC1 (tre-2/USP6, BUB2, cdc16) domain family, member 1	NM_015173	4p14	Hs.176503	−0.504146	1.17E−05*
2	*C10orf79*	Chromosome 10 open reading frame 79	NM_025145	10q25.1	Hs.288927	−0.503045	1.23E−05*
2	*SESN1*	Sestrin 1	NM_014454	6q21	Hs.591336	−0.502422	1.27E−05*
2	*NEK11*	NIMA (never in mitosis gene a)-related kinase 11	NM_145910	3q22.1	Hs.657336	−0.501333	1.33E−05*
3	*WDR19*	WD repeat domain 19	NM_025132	4p14	Hs.438482	−0.500027	1.41E−05*

Correlation coefficient and *P*-value indicate a representative data among multiple probes with eithe of two STC2 probes

* $P \leqq .05$

and correlation coefficient (0.57, $P = 3.44 \times 10^{-7}$), while the WD repeat domain 78 was inversely associated with *STC2* gene expression (−0.579, $P = 2.37 \times 10^{-7}$).

Clinical Significance of STC2 Expression in ESC: Expression of STC2 mRNA in Surgical Specimens

Of 70 clinical samples, 62 (88.5%) showed a higher expression level of *STC2* mRNA in cancerous tissues than in noncancerous tissues by real-time quantitative RT-PCR. The expression level of *STC2* mRNA in tumor tissues, 0.589 ± 0.759 (mean ± SD), was significantly higher than the 0.211 ± 0.444 in the corresponding normal tissues ($P <$ 0.0001, Fig. 2a). To investigate protein expression of *STC2,* immunohistochemical staining was performed 10 cases of the high *STC2* mRNA expression group. *STC2* is expressed in the cytoplasm and nuclei of cancer cells; however, it is not found in normal esophageal epithelium (Fig. 2b). Immunohistochemical analysis localized *STC2* expression specifically in cancer cells.

Clinicopathologic Significance of STC-2 mRNA Expression in ESC

The median expression levels of *STC2* mRNA in tumor tissues and normal tissues were 0.356 and 0.085, respectively. Patients with values less than the median expression level of 0.356 in tumor tissues were assigned to the low-expression group (n = 35). Those with values of >0.356 were assigned to the high-expression group (n = 35). Table 3 shows the clinicopathologic and *STC2* mRNA expression data in the tumor specimens from the 70 ESC patients. The incidence of lymph node metastasis was significantly higher ($P = 0.005$) in the high-expression group (28 of 35, 74.2%) than in the low-expression group (17 of 35, 48.6%). The incidence of lymphatic invasion was significantly higher ($P = 0.007$) in the high-expression group (28 of 35, 80.0%) than in the low-expression group (23 of 35, 65.7%). Moreover, the incidence of distant metastasis (category M of the tumor, node, metastasis system classification) was significantly higher ($P = 0.038$)

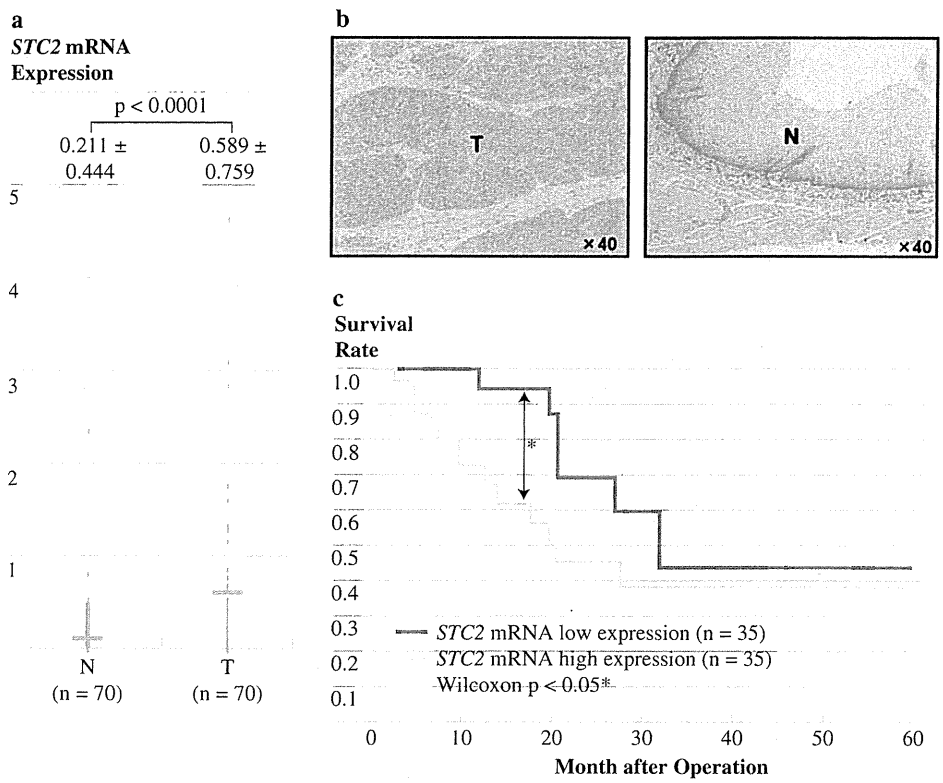

FIG. 2 **a** *STC2* (stanniocalcin 2) mRNA expression in cancer and noncancerous tissues from esophageal squamous-cell cancer (ESC) patients as assessed by quantitative real-time polymerase chain reaction (n = 70). *Horizontal lines* indicate the mean value of each group (N, noncancerous tissue; T, cancerous tissue). **b** Immunohistochemistry with *STC2* antibody on ESC patient samples. **a** Noncancerous tissue (original magnification, ×40). **b** Cancerous tissue, mRNA high-expression group (original magnification, ×40). **c** Kaplan–Meier disease-free survival curves for ESC patients according to the level of *STC2* mRNA expression. The survival rate for patients in the high-expression group was significantly higher than that for patients in the low-expression group ($P < 0.05$)

in the high-expression group (3 of 35, 98.6%) than in the low-expression group (0 of 31, 0.0%).

Relationship Between STC-2 mRNA Expression and Prognosis

The 5-year cause-specific survival rates in patients with high *STC2* mRNA levels and those with low *STC2* mRNA levels were 44.7 and 38.6%, respectively (Fig. 2c). The survival difference between these two groups was statistically significant (Wilcoxon, $P = 0.016$). Univariate analysis showed that the following factors were significantly related to postoperative survival: depth of invasion and lymph node metastasis, lymphatic invasion, and *STC2* expression ($P < 0.05$). Multivariate regression analysis indicated that depth of invasion and lymph node metastasis were independent prognostic factors, but *STC2* expression was not an independent prognostic factor (Table 4).

In Vitro Proliferation and Invasion Assays

To estimate whether high *STC2* expression affected cell growth rates, the *STC2* gene was transfected into the esophageal cancer cell line KYSE70 (Fig. 3a), and a proliferation assay was performed. As shown in Fig. 3b, there was a significant difference in the growth rate between *STC2*-transfected cells and mock-transfected cells ($P < 0.001$). In a clinicopathologic study, the incidence of lymphatic invasion and lymph node metastasis was significantly higher in the high-expression group than in the low-expression group. An in vitro Matrigel invasion assay confirmed these findings (Fig. 3c). The *STC2*-transfected cells exhibited significantly more invasive potential than the mock-transfected cells ($P < 0.001$), suggesting that high expression of *STC2* enhances tumor invasiveness and metastatic potential.

Effect of STC2 Gene Silencing

TE13 cells normally express *STC2* at a high level. Suppression of *STC2* mRNA was confirmed by quantitative RT-PCR (Fig. 3d). Protein expression was suppressed by *STC2*-specific RNAi as confirmed by Western blot analyses (Fig. 3e), with subsequent reduction in the proliferation rate of TE13 cells ($P < 0.001$) (Fig. 3f).

DISCUSSION

Among genes specifically overexpressed in cancer cells, 63 were previously associated with cancer progression. With respect to esophageal cancer, this study found overexpression of *SPP1, TAXTD1, ICAM1, HSP90,* and *MMP12* in addition to the *STC2* gene. *SPP1, BCAT1, APOE, LUM,* and *VIM* have been associated with

TABLE 3 Relationship between *STC2* expression and clinicopathologic findings

Characteristic	Total (n = 70)	STC2 expression		
		High expression n = 35 (50.0%)	Low expression n = 35 (50.0%)	*P*
Age (g) (mean ± SD)		66.5 ± 7.05	64.5 ± 10.98	NS
Sex				
Male	64	32 (91.4)	32 (91.4)	1.000
Female	6	3 (8.6)	3 (8.6)	
Histology				
Well	19	10 (31.2)	9 (25.7)	0.937
Moderate	38	19 (54.3)	19 (54.3)	
Poor	13	6 (14.5)	7 (20.0)	
pT				
pT1, T2	32	14 (40.0)	18 (51.4)	0.336
pT3, T4	38	21 (60.0)	17 (48.6)	
pN				
pN0	25	7 (20.0)	18 (51.4)	**0.005***
pN1	45	28 (74.2)	17 (48.6)	
pM				
pM0	67	32 (91.4)	35 (100.0)	**0.038***
pM1	3	3 (8.6)	0 (0.0)	
Lymphatic invasion				
Negative	20	5 (14.3)	15 (42.9)	**0.007***
Positive	50	30 (85.7)	20 (57.1)	
Venous invasion				
Negative	19	7 (20.0)	12 (34.3)	0.177
Positive	51	28 (80.0)	23 (65.7)	
Stage				
I, IIA	35	13 (37.2)	20 (57.1)	0.093
IIB, III, IV	35	22 (62.9)	15 (42.9)	

Bold values indicate * $P \leq .05$

TABLE 4 Univariate and multivariate analyses of clinicopathological factors affecting overall survival rate

Variable	n	5-year survival rate (%)	Univariate analysis, *P*	Multivariate analysis	
				Relative risk (95% CI)	*P*
Sex					
Male	64	44.7	0.115	–	–
Female	6	37.5			
Tumor depth					
pT1, 2	32	68.2	**0.035***	1.676	**0.043***
pT3, 4	38	24.3		(0.756–3.616)	
Lymph node metastasis					
Negative	25	72.6	**0.026***	2.023	**0.004***
Positive	45	27.9		(0.856–3.076)	
Lymphatic invasion					
Negative	20	85.7	**0.012***	–	–
Positive	50	29.1			
Venous invasion					
Negative	19	57.1	0.119	–	–
Positive	51	39.3			
STC2 expression					
Low	35	44.7	**0.016***	1.115	0.229
High	35	38.6		(0.658–2.020)	

95% CI 95% confidence interval

Bold values indicate * $P \leq .05$

metastasis not only in esophageal cancer, but also in other solid malignancies.[23–32] In comparison to other genes, *STC2* expression showed the most intimate correlation with clinicopathologic variables, such as lymphatic invasion, lymph node metastasis, and distant metastasis among those molecules in the esophageal cancer cases under study (data not shown). Therefore, we focused on *STC2* for further analysis, including functional studies, not only as a clinical prognostic marker of esophageal cancer, but also as a key molecule of esophageal cancer progression by the experiment of transfection of *STC2* and inhibition of *STC2* in vitro.

As for the mechanism of esophageal cancer cells related with *STC2* gene, we considered the function of *STC2* in normal mammalian tissues. It is reported that members of the STC family, *STC1* and *STC2*, regulate calcium and phosphate homeostasis.[33,34] Therefore, we examined the correlation between *STC2* and calcium metabolism-related molecules leading to malignancies.[35–39] However, expression profile in the current study did not indicate any significant correlation between *STC2* and those molecules. Therefore, the effect of *STC2* on the progression of esophageal cancer cell should be mediated through a function of other mechanisms apart from calcium metabolites.

Several additional studies have disclosed that *STC2* inhibits apoptosis by promoting the transcription of c-Myc and of hypoxia-induced factor (HIF)-1.[40–42] Hypoxia-induced *STC2* expression was found to be HIF-1 dependent, and *STC2* is a HIF-1 target gene that promotes cell proliferation in hypoxia.[43] There was no significant association between *STC2* and c-Myc or HIF-1 in the microarray analysis in the current study. Further studies are required to elucidate how *STC2* is involved in the progression of esophageal cancer cells.

In the current study, high *STC2* expression is correlated with poor prognosis, predominantly via lymph node metastases, and the forced expression of *STC2* and the knockdown of the *STC2* gene demonstrated that *STC2* was associated with ESC cellular proliferation and

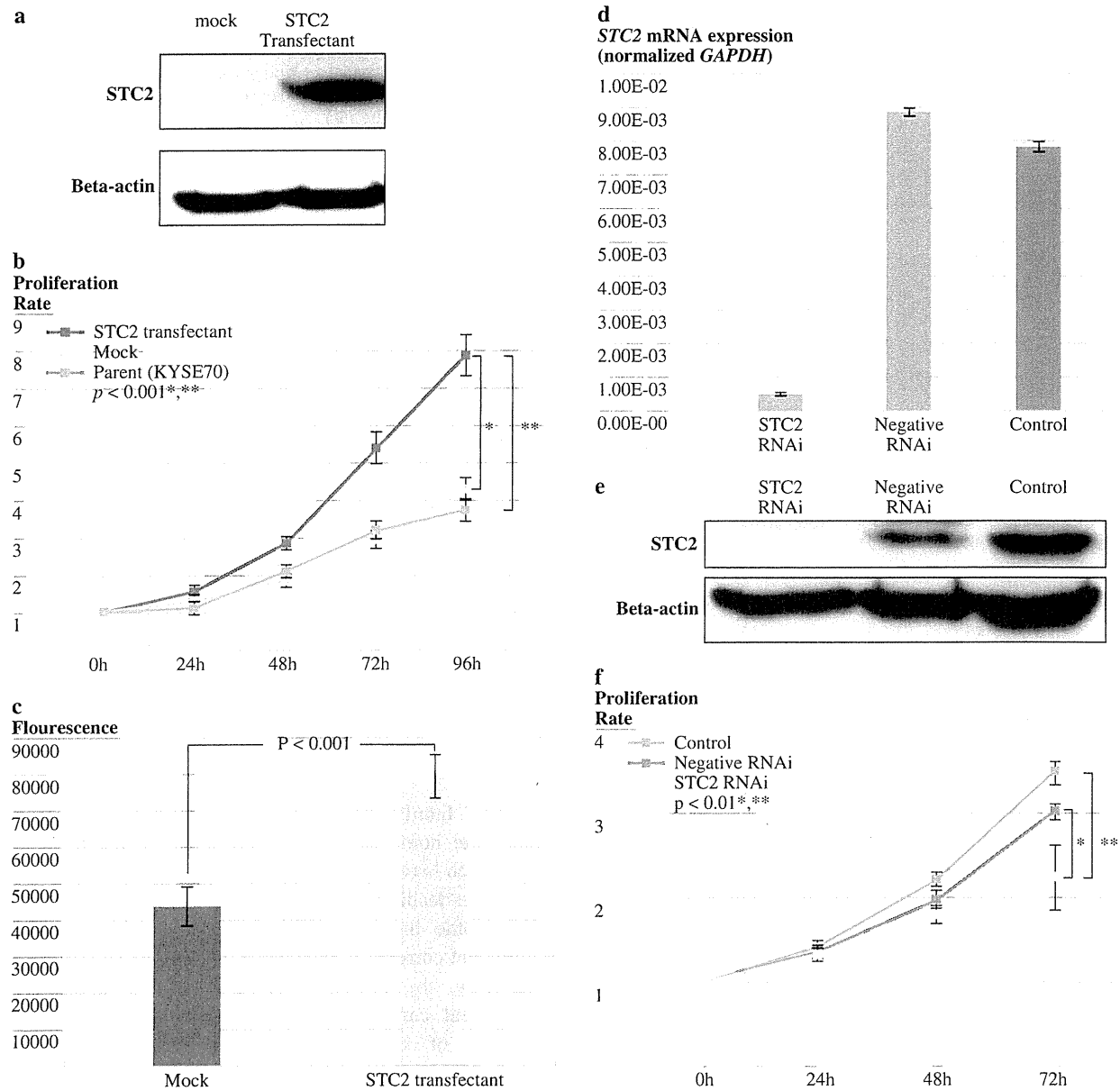

FIG. 3 **a** *STC2* (stanniocalcin 2) expression in *STC2*-transfected KYSE70 cells and mock-transfected KYSE70 cells. *STC2* expression was measured by Western blot analysis. **b** Proliferation of *STC2*-transfected cells and mock-transfected cells. *STC2*-transfected cells demonstrated increased proliferation compared to mock-transfected cells ($P < 0.001$). **c** The invasive potential of *STC2* transfected cells and mock-transfected cells. The *STC2*-transfected cells were more invasive than the mock-transfected cells ($P < 0.001$). **d**, **e** *STC2* expression suppressed by *STC2* specific-siRNA in TE13 cells. At 48 hours after siRNA addition, *STC2* expression was measured by quantitative real-time polymerase chain reaction (A) and Western blot analysis (B). **f** Effect of *STC2* suppression on TE13 cells proliferation as assessed by an MTT (3-(4,5-dimethylthiazol-2-yl)-2,5-diphenyl-tetrazolium bromide) assay. *STC2*-suppressed cells were less proliferative than control cells ($P < 0.01$)

invasiveness in vitro. The reason why ESC with high *STC2* expression shows aggressive behavior remains unclear; however, solid tumor progression is usually associated with hypoxia. There may be signals that corresponded with lymph node metastases in the signals that *STC2* stimulate.

In conclusion, this microarray study identified lymph node-specific, metastasis-related genes in esophageal cancer cells. Expression of one of the extracted genes, *STC2*, correlated with lymph node metastasis, lymphatic invasion, and poor prognosis. These findings suggest that *STC2* plays an important role in the behavior of esophageal cancer

cells. *STC2* expression may also be a predictor of survival in esophageal cancer patients. Further studies are needed to determine whether *STC2* represents a novel prognostic marker for esophageal cancer, a means of identifying patients who would benefit from postoperative adjuvant therapy, or a potential target for molecular therapy.

ACKNOWLEDGMENT Supported by CREST, Japan Science and Technology Agency; and the Japan Society for the Promotion of Science Grant-in-Aid for Scientific Research (Grants 21679006, 20390360, 20590313, 20591547, 21591644, 21592014, 20790960, and 21791297). We express our appreciation to T. Shimooka, K. Ogata, M. Oda, M. Kasagi, Y. Nakagewa, S. Matsuzaki, M. Kawamoto, Y. Fukuyoshi, A. Harada, Dr. N. Haraguchi, Dr. M. Ohkuma, Dr. K. Sakashita, Dr. Y. Takatsuno, Dr. K. Motoyama, Dr. T. Yokoe, Dr. Z. Xiang, Dr. Y. Kosaka, Dr. S. Hirasaki, Dr. K. Ishikawa, Dr. Y. Nakamura, and Dr. H. Sakashita for their technical assistance and advice.

CONFLICT OF INTEREST None.

REFERENCES

1. Sugimachi K, Matsuura H, Kai H, et al. Prognostic factors of esophageal carcinoma: univariate and multivariate analyses. *J Surg Oncol.* 1986;31:108–12.
2. Natsugoe S, Matsumoto M, Okumura H, et al. Prognostic factors in patients with submucosal esophageal cancer. *J Gastrointest Surg.* 2004;8:631–5.
3. Inoue H, Matsuyama A, Mimori K, Ueo H, Mori M. Prognostic score of gastric cancer determined by cDNA microarray. *Clin Cancer Res.* 2002;8:3475–9.
4. Mori M, Mimori K, Yoshikawa Y, et al. Analysis of the gene-expression profile regarding the progression of human gastric carcinoma. *Surgery.* 2002;131:S39–47.
5. Ohmachi T, Tanaka F, Mimori K, et al. Clinical significance of TROP2 expression in colorectal cancer. *Clin Cancer Res.* 2006;12:3057–63.
6. Mimori K, Kataoka A, Yoshinaga K, et al. Identification of molecular markers for metastasis-related genes in primary breast cancer cells. *Clin Exp Metastasis.* 2005;22:59–67.
7. Chang AC, Reddel RR. Identification of a second stanniocalcin cDNA in mouse and human: stanniocalcin 2. *Mol Cell Endocrinol.* 1998;141:95–9.
8. Welcsh PL, Lee MK, Gonzalez-Hernandez RM, et al. BRCA1 transcriptionally regulates genes involved in breast tumorigenesis. *Proc Natl Acad Sci USA.* 2002;99:7560–5.
9. Esseghir S, Kennedy A, Seedhar P, et al. Identification of NTN4, TRA1, and STC2 as prognostic markers in breast cancer in a screen for signal sequence encoding proteins. *Clin Cancer Res.* 2007;13:3164–73.
10. Buckanovich RJ, Sasaroli D, O'Brien-Jenkins A, et al. Tumor vascular proteins as biomarkers in ovarian cancer. *J Clin Oncol.* 2007;25:852–61.
11. Meyer HA, Tolle A, Jung M, et al. Identification of stanniocalcin 2 as prognostic marker in renal cell carcinoma. *Eur Urol.* 2009;55:669–78.
12. Staehler M. Editorial comment on: Identification of stanniocalcin 2 as prognostic marker in renal cell carcinoma. *Eur Urol.* 2009;55:678.
13. Tamura K, Furihata M, Chung SY, et al. Stanniocalcin 2 overexpression in castration-resistant prostate cancer and aggressive prostate cancer. *Cancer Sci.* 2009;100:914–9.
14. Volland S, Kugler W, Schweigerer L, Wilting J, Becker J. Stanniocalcin 2 promotes invasion and is associated with metastatic stages in neuroblastoma. *Int J Cancer.* 2009;125:2049–57.
15. Sobin LH, Fleming ID. TNM classification of malignant tumors. 5th ed. Union Internationale Contre le Cancer and the American Joint Committee on Cancer. *Cancer.* 1997;80:1803–4.
16. Utsunomiya T, Okamoto M, Hashimoto M, et al. A gene-expression signature can quantify the degree of hepatic fibrosis in the rat. *J Hepatol.* 2004;41:399–406.
17. Nishida K, Mine S, Utsunomiya T, et al. Global analysis of altered gene expressions during the process of esophageal squamous cell carcinogenesis in the rat: a study combined with a laser microdissection and a cDNA microarray. *Cancer Res.* 2005;65:401–9.
18. Brazma A, Hingamp P, Quackenbush J, et al. Minimum information about a microarray experiment (MIAME)—toward standards for microarray data. *Nat Genet.* 2001;29:365–71.
19. Hochberg Y, Benjamini Y. More powerful procedures for multiple significance testing. *Stat Med.* 1990;9:811–8.
20. Arigami T, Natsugoe S, Uenosono Y, et al. Lymphatic invasion using D2–40 monoclonal antibody and its relationship to lymph node micrometastasis in pN0 gastric cancer. *Br J Cancer.* 2005;93:688–93.
21. Ogawa K, Utsunomiya T, Mimori K, et al. Clinical significance of human kallikrein gene 6 messenger RNA expression in colorectal cancer. *Clin Cancer Res.* 2005;11:2889–93.
22. Shibata K, Tanaka S, Shiraishi T, Kitano S, Mori M. G-protein gamma 7 is down-regulated in cancers and associated with p 27kip1-induced growth arrest. *Cancer Res.* 1999;59:1096–101.
23. Ito T, Hashimoto Y, Tanaka E, et al. An inducible short-hairpin RNA vector against osteopontin reduces metastatic potential of human esophageal squamous cell carcinoma in vitro and in vivo. *Clin Cancer Res.* 2006;12:1308–16.
24. Kita Y, Natsugoe S, Okumura H, et al. Expression of osteopontin in oesophageal squamous cell carcinoma. *Br J Cancer.* 2006;95:634–8.
25. Xi L, Luketich JD, Raja S, et al. Molecular staging of lymph nodes from patients with esophageal adenocarcinoma. *Clin Cancer Res.* 2005;11:1099–109.
26. Hosch SB, Izbicki JR, Pichlmeier U, et al. Expression and prognostic significance of immunoregulatory molecules in esophageal cancer. *Int J Cancer.* 1997;74:582–7.
27. Akimoto T, Nonaka T, Harashima K, et al. Radicicol potentiates heat-induced cell killing in a human oesophageal cancer cell line: the Hsp90 chaperone complex as a new molecular target for enhancement of thermosensitivity. *Int J Radiat Biol.* 2004;80:483–92.
28. Ding Y, Shimada Y, Gorrin-Rivas MJ, et al. Clinicopathological significance of human macrophage metalloelastase expression in esophageal squamous cell carcinoma. *Oncology.* 2002;63:378–84.
29. Yoshikawa R, Yanagi H, Shen CS, et al. ECA39 is a novel distant metastasis-related biomarker in colorectal cancer. *World J Gastroenterol.* 2006;12:5884–9.
30. Oue N, Hamai Y, Mitani Y, et al. Gene expression profile of gastric carcinoma: identification of genes and tags potentially involved in invasion, metastasis, and carcinogenesis by serial analysis of gene expression. *Cancer Res.* 2004;64:2397–405.
31. Seya T, Tanaka N, Shinji S, et al. Lumican expression in advanced colorectal cancer with nodal metastasis correlates with poor prognosis. *Oncol Rep.* 2006;16:1225–30.
32. Hu L, Lau SH, Tzang CH, et al. Association of Vimentin overexpression and hepatocellular carcinoma metastasis. *Oncogene.* 2004;23:298–302.
33. Wagner GF, Jaworski E. Calcium regulates stanniocalcin mRNA levels in primary cultured rainbow trout corpuscles of stannius. *Mol Cell Endocrinol.* 1994;99:315–22.

34. Deol HK, Varghese R, Wagner GF, Dimattia GE. Dynamic regulation of mouse ovarian stanniocalcin expression during gestation and lactation. *Endocrinology.* 2000;141:3412–21.
35. Hardingham GE, Fukunaga Y, Bading H. Extrasynaptic NMDARs oppose synaptic NMDARs by triggering CREB shut-off and cell death pathways. *Nat Neurosci.* 2002;5:405–14.
36. Raya A, Kawakami Y, Rodriguez-Esteban C, et al. Notch activity acts as a sensor for extracellular calcium during vertebrate left-right determination. *Nature.* 2004;427:121–8.
37. Stolk M, Leon-Ponte M, Merrill M, Ahern GP, O'Connell PJ. IP3Rs are sufficient for dendritic cell Ca^{2+} signaling in the absence of RyR1. *J Leukoc Biol.* 2006;80:651–8.
38. Rossi D, Murayama T, Manini I, et al. Expression and functional activity of ryanodine receptors (RyRs) during skeletal muscle development. *Cell Calcium.* 2007;41:573–80.
39. Choi JH, Park JT, Davidson B, et al. Jagged-1 and Notch3 juxtacrine loop regulates ovarian tumor growth and adhesion. *Cancer Res.* 2008;68:5716–23.
40. Banasiak KJ, Xia Y, Haddad GG. Mechanisms underlying hypoxia-induced neuronal apoptosis. *Prog Neurobiol.* 2000;62: 215–49.
41. Maxwell PH, Pugh CW, Ratcliffe PJ. Activation of the HIF pathway in cancer. *Curr Opin Genet Dev.* 2001;11:293–9.
42. Ito D, Walker JR, Thompson CS, et al. Characterization of stanniocalcin 2, a novel target of the mammalian unfolded protein response with cytoprotective properties. *Mol Cell Biol.* 2004;24: 9456–69.
43. Law AY, Wong CK. Stanniocalcin-2 is a HIF-1 target gene that promotes cell proliferation in hypoxia. *Exp Cell Res.* 2010;316: 466–76.

Ann Surg Oncol (2011) 18:1166–1174
DOI 10.1245/s10434-010-1373-9

Annals of
SURGICAL ONCOLOGY
OFFICIAL JOURNAL OF THE SOCIETY OF SURGICAL ONCOLOGY

ORIGINAL ARTICLE – TRANSLATIONAL RESEARCH AND BIOMARKERS

Significance of Lgr5^{+ve} Cancer Stem Cells in the Colon and Rectum

Hidekazu Takahashi, MD[1], Hideshi Ishii, MD, PhD[1,2], Naohiro Nishida, MD[1,2], Ichiro Takemasa, MD, PhD[1], Tsunekazu Mizushima, MD, PhD[1], Masataka Ikeda, MD, PhD[1,2], Takehiko Yokobori, MD, PhD[2], Koshi Mimori, MD, PhD[2], Hirofumi Yamamoto, MD, PhD[1], Mitsugu Sekimoto, MD, PhD[1], Yuichiro Doki, MD, PhD, FACS[1], and Masaki Mori, MD, PhD, FACS[1,2]

[1]Department of Gastroenterological Surgery, Osaka University Graduate School of Medicine, Osaka, Japan; [2]Department of Molecular and Cellular Biology, Division of Molecular and Surgical Oncology, Kyushu University, Medical Institute of Bioregulation, Ohita, Japan

ABSTRACT

Purpose. Although recent studies show that leucine-rich repeat-containing G-protein-coupled receptor 5 (Lgr5)$^{+ve}$ cells targeted by Wnt drive self-renewal in the skin and gastrointestinal organs, the clinicopathological significance of Lgr5^{+ve} cancer stem cells (CSCs) of the colon remains to be elucidated.

Experimental Design. We studied the Wnt-targeted Lgr5 pathway in colorectal cancer (CRC). The expression of *LGR5*, *c-MYC*, *p21CIP1/WAF1/CDKN1A*, glutaminase (*GLS*), and miRs-23a and -23b (that target *LGR5* and *GLS*) was evaluated by quantitative real-time reverse-transcription polymerase chain reaction (RT-PCR). The Lgr5 protein was evaluated by immunohistochemistry. The clinical relevance of gene expression in terms of patient survival was also evaluated.

Results. Overexpression of *LGR5* was significantly associated with expression of *c-MYC*, *p21CIP1/WAF1/CDKN1A*, and *GLS* ($p < 0.0001$), and inversely associated with miR-23a/b ($p < 0.05$). Immunohistochemical analysis indicated that Lgr5 may be embedded in benign adenomas, localized at the tumor–host interface, and detectable over a broad area in established tumors. High level of *LGR5* expression was associated with poor prognosis for CRC cancer patients (disease-free survival; $p < 0.05$).

Conclusions. This study supports a significant role for *LGR5* in the CSC hypothesis in CRC: (1) Lgr5^{+ve} CSCs, presumably derived from normal stem cells in colonic crypts, proliferate, and the gene is overexpressed during CRC development; (2) *LGR5* expression is associated with activation of Wnt pathway, including oncogenic *c-MYC* and high energy production via glutaminolysis; (3) *LGR5* expression may be a poor prognostic factor for CRC patients. Further study of *LGR5* should contribute to the development of CSC-based cancer therapeutics.

First Received: 15 June 2010;
Published Online: 2 December 2010

M. Mori, MD, PhD, FACS
e-mail: mmori@gesurg.med.osaka-u.ac.jp

Human colorectal cancer (CRC) is one of the most extensively investigated tumor types.[1] Generally, stepwise accumulation of genetic and epigenetic alterations in oncogenes and tumor suppressor genes is considered the driving force behind malignancies. Recent models explain selected aspects of the complex process of CRC progression based on the hypothesis that many cancers are organized into hierarchies sustained by cancer stem cells (CSCs) at their apex.[2] This hypothesis has generated excitement in many quarters of the clinical cancer research community.[3] CSCs mimic normal adult stem cells by demonstrating resistance to toxic injuries and chemoradiation therapy, and they may be responsible for tumor relapse following apparently beneficial treatments as well as for invasion and metastasis.[2] In CRC, several cell-surface markers have been reported to detect CSCs, including CD24, CD29, CD44, CD133, CD166, the epithelial cell adhesion molecule (Ep-CAM), also known as epithelial-specific antigen (ESA), and the leucine-rich repeat-containing G-protein-coupled receptor 5 (Lgr5), also known as Gpr49 (Table 1).[4–6]

Previous studies on CSC incidence in primary CRC indicated the marked prognostic influence of CD133, but not vascular endothelial or epidermal growth factor receptor, on metastasis and its positive association with

5′-TGCAGAGGGTCATGTTGAAG-3′, antisense primer 5′-CATCCATGGGAGTGTTATTCC-3′; and *VIM* (NM_003380.3) sense primer 5′-AAAGTGTGGCTGCCAAGAAC-3′, antisense primer 5′-AGCCTCAGAGAGGTCAGCAA-3′. To confirm RNA quality, the glyceraldehyde-3-phosphate dehydrogenase (*GAPDH*) gene served as internal control. The sequences of the *GAPDH* primers were as follows: sense primer 5′-TTGGTATCGTGGAAGGACTCA-3′, antisense primer 5′-TGTCATCATATTTGGCAGGTT-3′. The amplification protocol included initial denaturation at 95°C for 10 min, followed by 45 cycles of 95°C for 10 s and of 60°C for 30 s. PCR was performed in a LightCycler 480 system (Roche Applied Science) using the LightCycler 480 Probes Master kit (Roche Applied Science). All concentrations were calculated relative to the concentration of cDNA from Human Universal Reference total RNA (Clontech). The concentration of *LGR5* was then divided by the concentration of the endogenous reference (*GAPDH*) to obtain normalized expression values. For miR-23a/b and miR-200c qRT-PCR, cDNA was synthesized from total RNA using TaqMan MicroRNA miR-23a/b and miR-200c specific primers (Applied Biosystems, Foster City, CA, USA) and a TaqMan MicroRNA Reverse Transcription kit (Applied Biosystems). qRT-PCR was performed in the LightCycler 480 system using the LightCycler 480 Probes Master kit. The following temperature profile was used: initial denaturation at 95°C for 10 min, followed by 45 cycles of 95°C for 10 s and of 60°C for 30 s. Expression levels of target miRNAs were normalized to that of a small nuclear RNA RNU6B (Applied Biosystems) transcript.

Immunohistochemistry

Immunohistochemical analyses of Lgr5 were performed using surgical specimens from selected patients with CRC at Osaka University. The avidin–biotin–peroxidase method (Vectastain Elite ABC reagent kit; Vector) was used on formalin-fixed, paraffin-embedded tissues. After deparaffinization and blocking, the antigen–antibody reaction was carried out overnight at 4°C. The Vectastain Elite ABC reagent kit was used to detect the signal of the Lgr5 antigen–antibody reaction. Rabbit polyclonal antibody against the human Lgr5 loop 2 domain (Abgent, San Diego, CA, USA) was used at 1:20 and against the human Lgr5 cytoplasmic domain (MBL International, Nagoya, Japan) at 1:50 dilution.

Statistical Analysis

Statistical analyses were performed using JMP 8.0.1 (SAS Institute) for Windows. Possible differences between groups were analyzed using Student's *t*-test, χ^2 test, or Wilcoxon test. The association between expression levels of gene messenger RNA (mRNA) and miR family was analyzed using the Pearson correlation coefficient. Survival curves were obtained by the Kaplan–Meier method; comparison between curves was completed by log-rank test. Probability level of 0.05 was chosen to indicate statistical significance.

RESULTS

LGR5 was Preferentially Overexpressed in CRC

We performed RT-PCR analysis using paired primary and adjacent noncancerous CRC regions. Clinicopathological evaluation showed statistically significant differences between groups with high and low *LGR5* expression (classified as having expression levels higher or lower than the median value, respectively). Significant between-group differences were observed in lymph node metastasis (Student's *t*-test, $p = 0.034$), liver metastasis ($p = 0.0245$), and age ($p = 0.039$). One hundred eighty paired primary tumor samples were studied using quantitative real-time RT-PCR. The data showed that the mean expression value of *LGR5* mRNA in tumor tissues was significantly higher than that for corresponding paired normal tissues ($p < 0.0001$; Student's *t*-test; Fig. 1a).

Overexpression of LGR5 Is Associated with the Oncogene c-MYC in CRC

The Wnt-targeted *Lgr5* gene has recently been identified as a novel stem cell marker in the intestinal epithelium and in hair follicles.[13–15] Recent studies have indicated that Wnt signaling is influenced by the single-nucleotide polymorphism rs6983267, which maps to 8q24, and serves as an enhancer of *c-MYC* expression through binding of T-cell factor-4 (Tcf4).[16] We studied the correlation between *LGR5* expression and *c-MYC* mRNAs. Data from quantitative real-time RT-PCR of 89 paired primary tumor samples indicated that *LGR5* expression in patients with high *c-MYC* expression was higher than that in patients with low *c-MYC* expression ($p < 0.0001$; Fig. 1b). The expression of *LGR5* mRNAs was also associated with *c-MYC* mRNAs ($R = 0.744$; Fig. 1c), suggesting the clinical relevance of *LGR5* and *c-MYC* transcription in co-overexpression downstream of the common pathway of Tcf4 targets.[17]

Overexpression of LGR5 and c-MYC Genes Reciprocally Associated with Differentiation Mediator p21CIP1/WAF1/CDKN1A

Disruption of oncogenic β-catenin/Tcf4 activity induces rapid G1 arrest and intestinal differentiation via

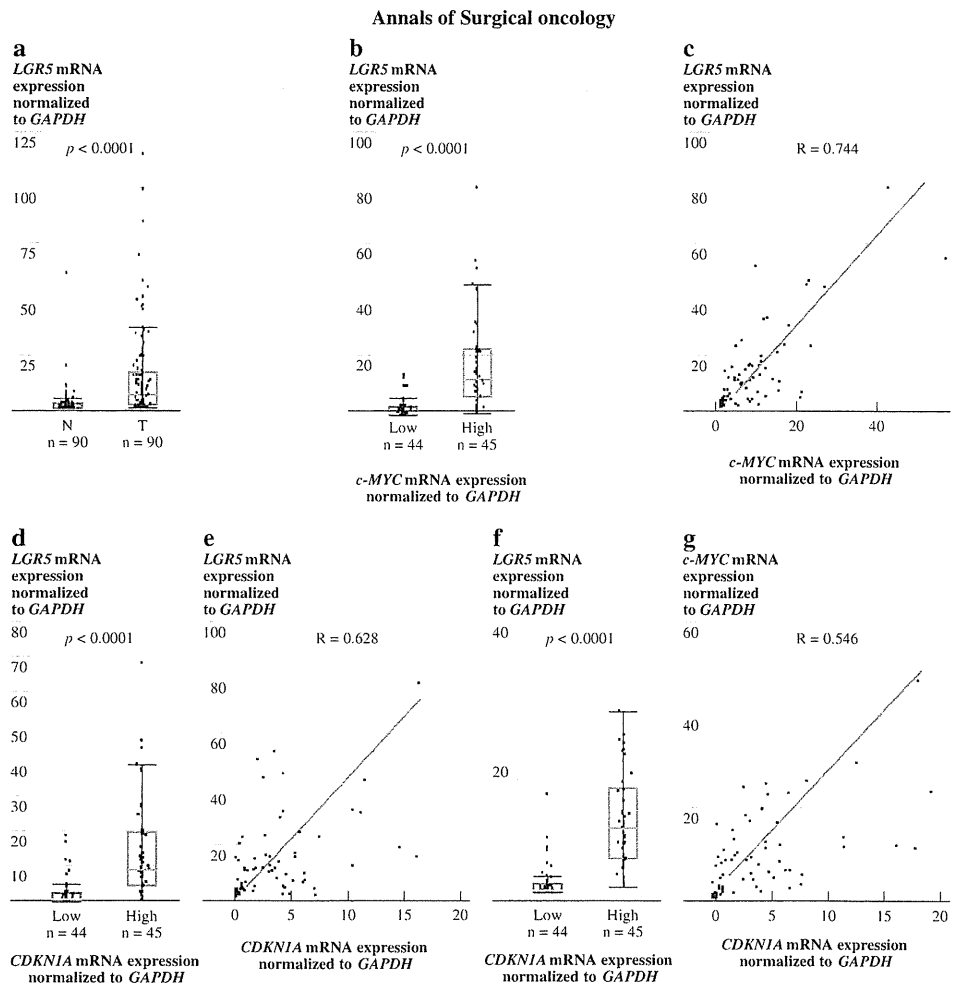

FIG. 1 Overexpression of *LGR5* was associated with increased expression of the oncogene *c-MYC* and of *p21CIP1/WAF1/CDKN1A* in 89 subjects with CRC. Expression was evaluated by the ratio normalized to *GAPDH* expression. **a** Expression of *LGR5* was increased in tumor (T) compared with normal (N) samples ($p < 0.0001$). **b**, **c** Increased expression of *c-MYC* was associated with an increase in *LGR5* expression (**b**, $p < 0.0001$; **c**, $R = 0.744$). **d**, **e** Association of *p21CIP1/WAF1/CDKN1A* expression with *LGR5* expression (**d**, $p < 0.0001$; **e**, $R = 0.628$). **f**, **g** Association of *p21CIP1/WAF1/CDKN1A* expression with *c-MYC* expression (**f**, $p < 0.0001$; **g**, $R = 0.564$). In **b**, **d**, and **f**, the 89 subjects were classified into two groups, those with high and low levels of expression, and the results are shown against *LGR5* (**d**) and *c-MYC* (**f**) expression. In **c**, **e**, and **g**, a linear association was shown between *LGR5* and *c-MYC* (**c**) and (**e**), and between *c-MYC* and *p21CIP1/WAF1/CDKN1A* (**g**)

transcriptional activation of a cyclin-dependent kinase inhibitor encoding the *p21CIP1/WAF1/CDKN1A* gene.[13] We hypothesized that the involvement of this switch mechanism in cancer development (i.e., expression of the *p21CIP1/WAF1/CDKN1A* gene) is deregulated under the co-activation of the *LGR5* and *c-MYC* genes in CRC, but it is not related to terminal differentiation, which is characteristic of cancer cells. In the present study, *LGR5* expression in patients with overexpression of *p21CIP1/WAF1/CDKN1A* was higher than in patients with low *p21CIP1/WAF1/CDKN1A* expression ($p < 0.0001$; Fig. 1d); the expression of *LGR5* mRNAs was associated with that of the *p21CIP1/WAF1/CDKN1A* mRNAs ($R = 0.628$; Fig. 1e). Similarly, quantitative real-time RT-PCR indicated that *c-MYC* expression in patients with overexpression of *p21CIP1/WAF1/CDKN1A* was also higher than that in patients with low *p21CIP1/WAF1/CDKN1A* expression ($p < 0.0001$; Fig. 1f); the expression of *c-MYC* mRNAs was associated with that of the *p21CIP1/WAF1/CDKN1A* mRNAs ($R = 0.546$; Fig. 1g). The present study demonstrated that the Wnt targets, genes *LGR5* and *c-MYC*, are co-activated in CRC and are associated with reciprocal activation of *p21CIP1/WAF1/CDKN1A*, suggesting that Wnt oncogenic signals may antagonize a cyclin-dependent kinase inhibitor, inducing cell cycle arrest and differentiation in CRC.

In Situ Expression Pattern of the Lgr5 Protein in Adenomas and Carcinomas

Progression of malignant tumors in CRC, namely from adenoma to early carcinoma in situ, to established carcinoma, and finally to dissemination of tumor cells (a prerequisite for metastasis), is correlated with loss of epithelial differentiation and acquisition of a migratory phenotype.[18] However, Lgr5^{+ve} normal stem cells are speculated to be localized in the basal crypt area of the normal colon mucosa.[17] Lgr5^{+ve} CSCs may be embedded in benign adenomas, localized at the tumor–host interface, and detectable over a broad area in established tumors. To

test this, immunohistochemical staining with anti-Lgr5 antibody against the extracellular loop 2 domain was performed. The antibody was detected in active crypt base columnar (CBC) cells (representing intestinal stem cells at the crypt bottom), and the stain was detected in the upstream neck region of the crypts (Fig. 2a). Similar results were obtained using another anti-Lgr5 antibody that was developed against the intracellular region (Fig. 2b). In the current study, we used the former antibody and then studied Lgr5 staining in adenomas. The results showed that Lgr5 expression was detected in peripheral crypt-like regions in which the CSCs were supposed to be located (Fig. 2d from Fig. 2c) but not in the central area of the polyps (Fig. 2e from Fig. 2c).[18] We then studied Lgr5 expression in carcinomas in situ, showing that $Lgr5^{+ve}$ cells were distributed in the crypt-like area at the tumor–host interface (Fig. 2i from Fig. 2g) and to a lesser extent in the lumen (Fig. 2h from Fig. 2g). Lgr5 expression was ubiquitous in established adenocarcinomas (Fig. 2j from Fig. 2i; Fig. 2k, a negative case). Considering the recent proposal concerning migratory CSCs (a variant distinct from stationary CSCs) and their ability to play a critical role in invasion and metastasis through mobilization to the invasive front, both CSC types may express the Lgr5 protein, suggesting that its expression may be relevant to the biological behavior of CSCs.

miR-23 Inversely Associated with LGR5 and GLS Expression

Recently, it was reported that c-Myc transcriptionally represses miR-23a/b, resulting in greater expression of their target protein, mitochondrial glutaminase (Gls) (Fig. 3g).[19] miRs are short ~22-nucleotide RNA sequences that bind to complementary sequences of multiple target mRNAs, usually resulting in their silencing mainly at

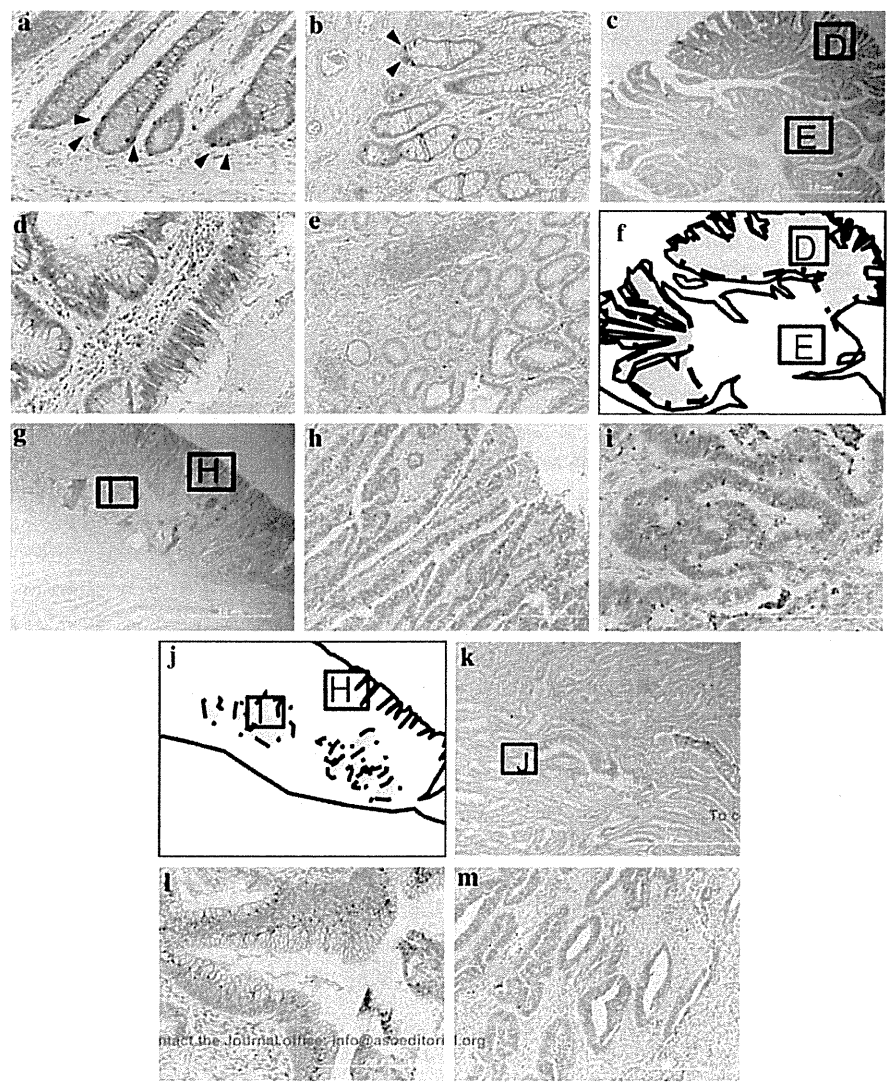

FIG. 2 Sequential detection of $Lgr5^{+ve}$ cells in normal mucosa, adenoma, carcinoma in situ, and advanced carcinoma by immunohistochemical staining. **a**, **b** Lgr5 staining in normal colonic mucosa. a, detected by antibody against the extracellular loop 2 domain of Lgr5; b, detected by antibody against the cytoplasmic region of Lgr5. **c–e** Lgr5 staining in an adenomatous polyp of the colon. Positive stain was detected in the peripheral region of each polyp lobe (**d**) but not in the central region of the polyp (**e**), suggesting a degree of central differentiation and peripheral localization of $Lgr5^{+ve}$ CSCs. **f** Schematic representation of C. $Lgr5^{+ve}$ cells were localized to the peripheral region (*shaded*). **g–i** Lgr5 staining in carcinoma in situ. Positive stain was detected in the tumor–host interface regions in the carcinoma (**i**) but not at the surface (**h**). **j** Schematic representation of g. $Lgr5^{+ve}$ cells located at the tumor–host interface region (shaded). **k**, **l** Lgr5 staining in advanced carcinoma. Positive staining was ubiquitous. **m** A CRC case with absence of Lgr5 expression as the control

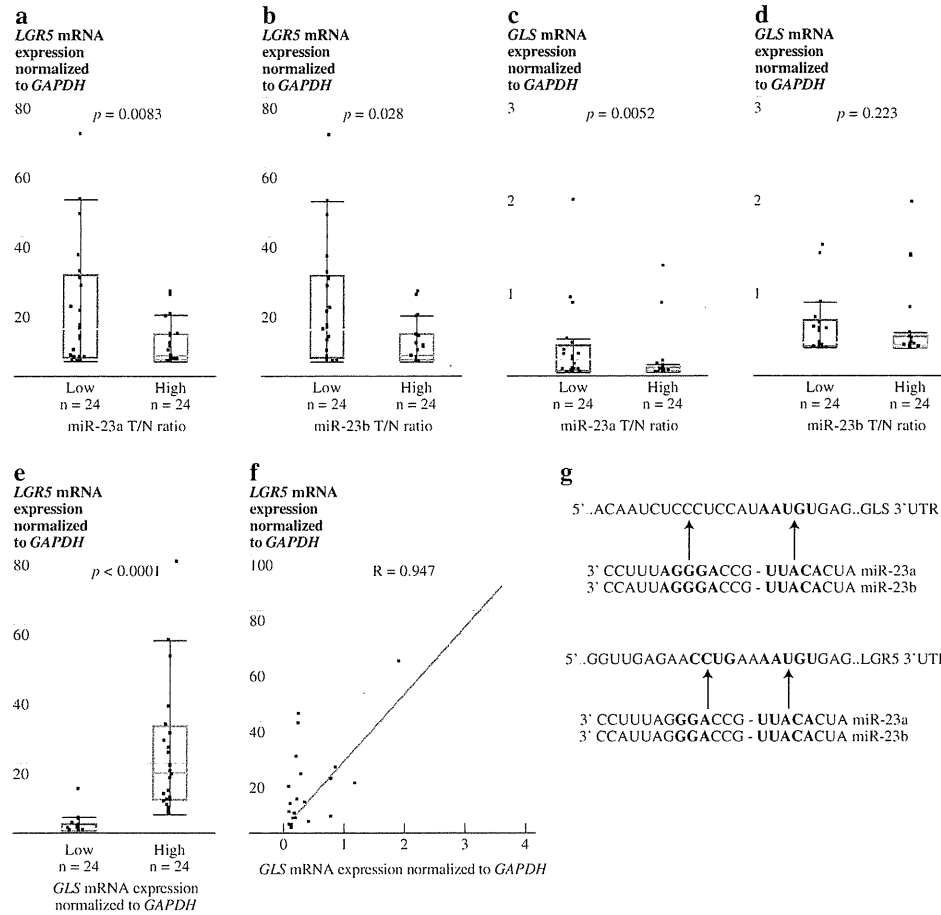

FIG. 3 Inverse correlation between *LGR5* and a *c-MYC* target, miR-23a/b. Expression was evaluated by the ratio normalized to *GAPDH* expression. *LGR5* and *GLS* expression in 48 subjects (two groups, those with high and low levels of expression) shown against miR-23a (**a**, **c**; both $p < 0.05$) and miR-23b (**b**, $p < 0.05$; **d**, $p = 0.223$) expression. The data suggest the candidacy as a target of miR-23 family to *LGR5*. **e**, **f** Expression of *LGR5* mRNA is shown against *GLS* expression (**e**, $p < 0.05$; **f**, $R = 0.947$). **g** Schematic representation of the miR-23 family relative to the *LGR5* and *GLS* genes

translation level as well as by involvement of posttranscriptional regulation.[20] miRs target ~60% of all genes, and several miRs are associated with some types of cancer.[21,22] The candidate approach to nucleotide sequence analysis using a web-based search program for identifying predicted miR targets for *LGR5* in mammals (http://www.targetscan.org/) enabled identification of miR-23a/b (Fig. 3g). Quantitative real-time RT-PCR of 48 samples indicated that *LGR5* expression in patients with high miR-23a levels was lower than that among patients with low miR-23a levels ($p < 0.01$; Fig. 3a). *LGR5* expression in patients with high miR-23b levels was lower than that among patients with low miR-23b levels ($p < 0.05$; Fig. 3b), indicating an inverse correlation between expression of *LGR5* and miR-23a/b. The expression analysis indicated that *GLS* expression in patients with high miR-23a levels was lower than that among patients with low miR-23a levels ($p < 0.01$; Fig. 3c); however, this difference was not significant for miR-23b levels ($p = 0.223$; Fig. 3d). *LGR5* expression was associated with *GLS* expression (Fig. 3e, f).

High LGR5 Expression Associated with Poor Disease-Free Survival

Kaplan–Meier estimation of overall survival of all patients in the present study indicated no significant association with expression of *LGR5* (Fig. 4a). We next hypothesized that the remaining Lgr5^{+ve} cells in unresected lesions affected the prognosis of patients; therefore, we selected cases in which patients received radical surgery. The overall survival of this series of patients indicated a tendency toward poor prognosis in those with high *LGR5* levels (Fig. 4b). On the other hand, the disease-free survival of the above selected cases (as shown in Fig. 4b) indicated that high *LGR5* expression was significantly associated with poor prognosis (Fig. 4c; log-rank $p < 0.05$). The association of other factors, such as *p21CIP1/WAF1/CDKN1A*, *GLS*, and miR-23a/b, with patient survival was not significant ($p > 0.05$; data not shown). The present study suggests that the expression level of *LGR5* is a prognostic factor of the natural course of CRC.

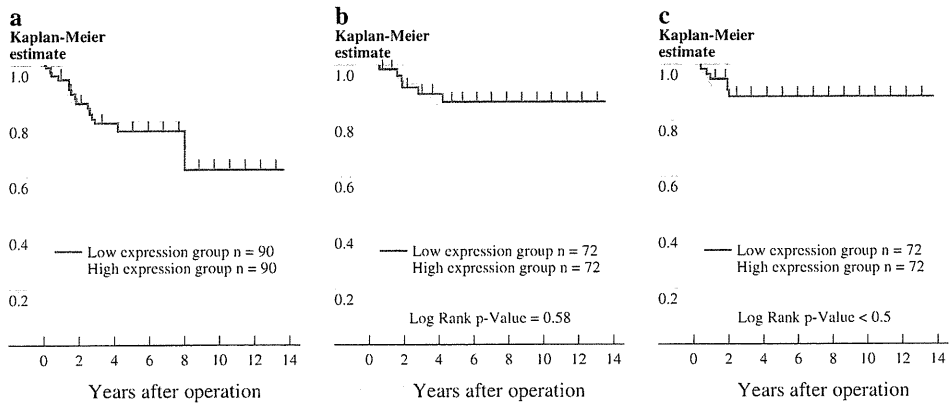

FIG. 4 Survival curves for LGR5-positive and LGR5-negative subjects. **a** Overall survival for all 180 subjects (two groups, those with high and low expression of LGR5). No significant between-group difference was detected. **b** Overall survival for subjects who underwent radical tumor resection (two groups, those with high and low expression of LGR5). No significant between-group difference was detected. **c** Disease-free survival of subjects who underwent radical tumor resection (two groups, those with high and low expression of LGR5). A significant between-group difference was observed ($p < 0.05$)

miR-200c Inversely Associated with LGR5 and VIM Expression

Recently, it was reported that epithelial–mesenchymal transition (EMT) is closely related with migration and metastasis of cancer cells.[18] EMT is also induced by Wnt signaling in CRCs.[23] Activation of Wnt/β-catenin pathway might trigger EMT and acquisition of mesenchymal molecules such as VIM.[24] miR-200c was reported as an inducer of epithelial differentiation and inversely related to EMT.[25] Quantitative real-time RT-PCR of 48 samples indicated that *LGR5* expression in patients with high *VIM* levels was higher than that among patients with low *VIM* levels ($R = 0.543$, $p < 0.0001$; Fig. 5c), indicating a correlation between expression of *LGR5* and *VIM*. *LGR5* expression in patients with high miR-200c levels was lower than that among patients with low miR-200c levels ($R = -0.175$, $p = 0.0042$; Fig. 5d), indicating an inverse correlation between expression of *LGR5* and miR-200c.

DISCUSSION

Although the exact time point at which the concept of CSCs (i.e., the concept that malignant tumors arise from a small population of multipotent cells harboring the ability to self-renew) is a matter of debate, Furth and Kahn had reported in 1937 that a single cell could give rise to leukemia in mice.[26] Thereafter, the development of flow cytometry enabled identification of a small population harboring tumor-initiating activity, and a line of experimental data was provided in 1997 showing that human acute leukemia can be organized as a hierarchy that originates from a primitive hematopoietic cell.[2,27,28] Because the characterization of rare CSCs in leukemia shows intrinsic drug efflux capacity, molecular markers for detection of CSCs have been reported in solid tumors of the head, neck, gastrointestinal system, colon, breast, and brain.[27,29–36] These relatively small populations of CSCs are potentially important because they may play a role in resistance to chemotherapy and radiation therapy and appear to be responsible for cancer recurrence after treatment, even when most of the cancer cells appear to have been destroyed.[37]

The present findings suggest the significance of $Lgr5^{+ve}$ CSCs. The Lgr5 protein, an orphan seven-transmembrane-domain receptor similar to the thyroid-stimulating hormone, follicle-stimulating hormone, and luteinizing hormone receptors, was identified as a Wnt/Tcf4 target gene expressed in CRC.[13,38] Lgr5 marks rapidly cycling stem cells in the small intestine and colon as well as hair follicles.[14,15] The control of self-renewal in intestinal crypts and hair follicles shares many regulatory characteristics, including a prominent role of the Wnt cascade.[39] The present data indicate that the Wnt targets, *LGR5* and *c-MYC*, are overexpressed in CRC, demonstrating an oncostimulating function of this pathway in CRC development and the possibility that Lgr5 is a surface marker of CSCs.

The Lgr5 protein was markedly expressed in the peripheral regions of adenomas and at the invasive front (the tumor–host interface); it was also detectable over a broad area in established tumors. This distribution of $Lgr5^{+ve}$ cells suggests that accumulation of genome mutation affects the location and polarity of $Lgr5^{+ve}$ stem cells, during tumor establishment in the adenoma–carcinoma sequence (Fig. 5b). The fact that the distribution of Lgr5 protein is not restricted to the apical surface suggests that hypertranslation or abnormal form of the Lgr5 protein